ARTICLE NO. 78-209R

Flow about a Propeller-Driven Body in Temperature-Stratified Fluid

T. F. Swean Jr.* and J. A. Schetz†
Virginia Polytechnic Institute and State University, Blacksburg, Va.

An experimental study of the turbulent flowfield produced by a slender, stern-propeller-driven body in a temperature-stratified fluid is presented. The testing was conducted in the Virginia Polytechnic Institute 2 m × 2 m subsonic wind tunnel at $Re_D \approx 2 \times 10^5$. The temperature stratification was produced by upstream injection of heated air in a manner such that a uniform approach velocity field was retained. The temperature variation provided a means of tracing flow development in the near-body region. Mean flow velocities, static pressure, flow angularity, and mean temperature distributions are reported at five downstream stations: $Z/D = 0.33$, 1.0, 2.0, 3.0, and 4.0. Turbulence data, including temperature fluctuations, are reported at $Z/D = 0.33$ and $Z/D = 4.0$. The principal effect of the propeller was to induce a more or less rigid rotation immediately downstream of the body. No significant increase in mixing rate was observed to be produced by the propeller in the region up to 4.0 body diameters downstream. Temperature fluctuation was low across the wake, except in the vicinity of the propeller tips where it became relatively large. The high-temperature fluctuation often occurred in regions of low mean temperature gradients, which indicates that current turbulence modeling techniques might have to be re-examined.

Nomenclature

D	= body diameter
P	= pressure
R	= radial distance measured from the axis
Re_D	= Reynolds number based on diameter
T	= mean temperature
$\sqrt{T'^2}$	= temperature fluctuation
u	= axial velocity
$\sqrt{u'^2}$	= axial velocity fluctuation
$\sqrt{v'^2}$	= radial velocity fluctuation
$\overline{u'v'}$	= Reynolds stress
X	= horizontal distance measured from the axis
Y	= vertical distance measured from the axis in the direction opposite to the "sail"
Y'	= vertical distance measured from the body surface
Z	= downstream distance measured from the body tail
Z'	= downstream distance measured from the body nose
ρ	= density

Introduction

THE turbulent wake produced by a body in a fluid stream has long been a subject of interest in fluid mechanics. With a thorough understanding of wake development and subsequent dissipation, the problem of dispersion and control of pollutants from aircraft and water vehicle propulsion units can be approached better. Experimental studies of the turbulent wake are also of interest for testing theories of turubulent modeling.

Most of the previous experimental studies have dealt with relatively simple bodies in the unpropelled or "drag-body" situation. In fact, many estimates of the wake development behind self-propelled bodies have been based on the experiments of Naudascher,[1] in which the momentumless condition was established with a circular disk and a central jet providing the necessary thrust to balance the drag of the disk. Later, Gran[2] investigated the momentumless wake behind a self-propelled Rankine ovoid at $Re_D \approx 6 \times 10^4$. Extensive work was published in 1974 by Swanson et al.[3] and Chieng et al.[4] for a slender, propeller-driven body at $Re_D \approx 6 \times 10^5$. Daffan[5] extended the work of Swanson and Chieng by studying the effect of an appendage and nonzero pitch angles (0-2 deg). Schetz et al.[6] studied the effect of replacing the single propeller by an equivalent set of side-by-side counter rotating propellers.

The present investigation was designed to study the development of the body, propeller, and near-wake flow using fluid temperature as a tracer. The stratification of the temperature field remains sufficiently small, such that buoyancy effects are negligible.

The testing was conducted in the VPI 2 m × 2 m wind tunnel at $Re_D \approx 2 \times 10^5$. In order to achieve a temperature-stratified flow, an air injection and heating system was designed and built. The primary design criterion of the heating/injection

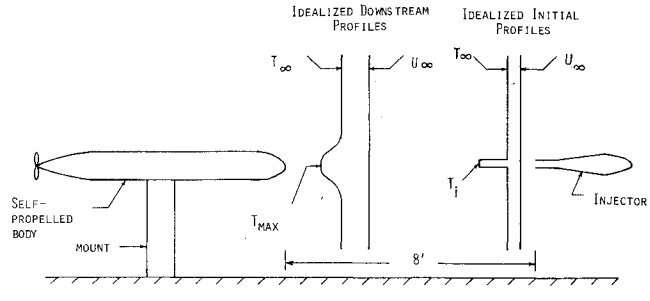

Fig. 1 Schematic of test section arrangement to produce the temperature-stratified approach flow.

Presented as Paper 78-209 at the AIAA 16th Aerospace Sciences Meeting, Huntsville, Ala., Jan. 16-18, 1978; submitted Feb. 8, 1978; revision received Feb. 28, 1979.

Index categories: Propulsion for Marine Applications; Jets, Wakes, and Viscid-Inviscid Flow Interactions; Marine Propulsion.

*Graduate Asst., Aerospace and Ocean Engineering Dept.; presently STD Inc., Washington, D.C.

†Professor and Dept. Head, Aerospace and Ocean Engineering Dept. Associate Fellow AIAA.

arrangement was to produce in the upstream wind-tunnel flow a slug of heated air, while disturbing the approach velocity field as little as possible.

This paper is arranged into several sections. First, the apparatus, models, and experimental methods are described in detail. The results are presented in separate sections, starting with the boundary-layer data. The next subsections deal with the mean wake flow, and finally the turbulence measurements in the near wake are reported. The results are presented here in graphical form; tabulated data are available from the authors.

Experimental Apparatus and Instrumentation

Wind-Tunnel Facility

All tests were conducted in the VPI subsonic stability tunnel at a dynamic pressure 2.54 cm of water (approximately 2.3 m/s), corresponding to a Re_D based on a diameter of 2.04×10^5.

Self-Propelled Model

The model used in this investigation has a maximum diameter of 15.2 cm and a fineness ratio of 12:1. The model was strut mounted from the floor of the wind-tunnel in the center of the test section. The forebody is parabolic and machined from laminated layers of plexiglass. The centerbody is an aluminum cylindrical tube. The tail body is also plexiglass machined into an ogival shape. The strut enters the body through a streamlined "sail."

The model used a 2.0 kW dc motor to direct-drive the single propeller shaft which extended through the center of the tail. A 15.2-cm-diam, 10.2-cm-pitch, three-bladed model airplane propeller, Tornado model manufactured by Grish Bros. was used to provide sufficient thrust to obtain the self-propelled condition (see Ref. 6 for further details of the model).

To avoid overheating in long duration experiments, the motor was enclosed by copper tubing to allow for water cooling. The water cooling was not used for the short duration test necessary to determine the required propeller speed to produce the momentumless condition. The "sail-drag" is included in determining this condition. In order to measure the forces and moments on the body, a strain gage balance was internally mounted in the model.

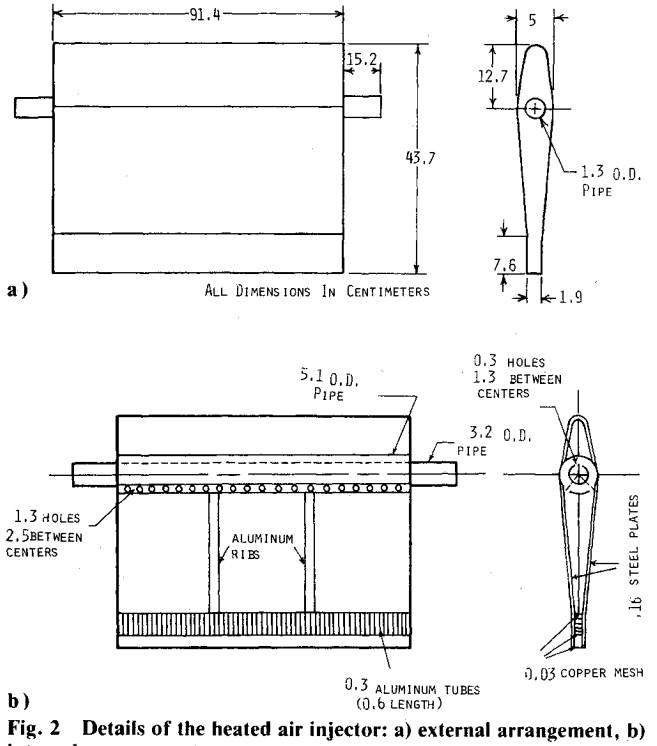

Fig. 2 Details of the heated air injector: a) external arrangement, b) internal arrangement.

Air Heating Apparatus

The stratification of the approaching airstream was induced by injecting heated air at the freestream velocity upstream of the self-propelled model. A schematic of the test section arrangement, including the injection and self-propelled model, is shown in Fig. 1. An injector was constructed with the overall dimensions shown in Fig. 2a. The interior of the injector is shown in Fig. 2b. Air enters the injector from both sides through a 2.5-cm pipe and exits through small holes that are distributed uniformly on the centerline along the span. Surrounding this pipe is a larger pipe in which two rows of 1.3 cm holes are evenly distributed along the span. These holes are offset above and below the centerline by 45 deg. Downstream of the pipe assembly there is a thin splitter plate to help guide the exiting air and begin the flow straightening process. Immediately downstream of this plate, the injector is filled with 0.3 cm, aluminum tubes of 3.2-cm length that are held in place by a small box. The upstream and downstream ends of this box are covered with copper mesh. The basic ideas for the construction of the injector were obtained from Hokenson.[7]

The injected air was supplied by four compressors operating continuously. The compressed air fed into a pressure regulator which controlled the mass flow rate. The heating was done electrically by six Plasmatron PS-20 transformers. The heating mechanism was as shown in Fig. 3. After leaving the regulator, the air was guided into two lengths of Inconel 601 3.2-cm-diam 0.6-cm wall pipe. The Plasmatrons were connected to the upstream and downstream ends of the pipes, thus forming a parallel electric circuit. To minimize the heat loss to the atmosphere, the entire piping system from the upstream end of the heating circuit to the injector was covered by insulation.

Wake Probes

The mean flow pressure measurements in the wake were taken using a five-port, three-dimensional yawhead probe. The output from the pressure probe was read on an electronic manometer. To read all five pressure points from the yawhead probe on the manometer, a Scanivalve fluid switch wafer was used. The mean temperature field was measured by means of a thermocouple.

The axial and radial turbulence and radial shear stress data were obtained using a crosswire probe (TSI model 1231T1.5). The probe was operated at an overheat ratio of 1.8 using a constant temperature anemometer module and a power supply and monitor. Readings were taken from a DISA meter. A correlator and a TSI voltmeter were also used. The probe was calibrated by orienting one of the sensors parallel to the flow direction and subjecting the probe to two different flow conditions (motionless air and air at 32 m/s). The probe was then rotated 90 deg to align the other sensor and the process was repeated. Temperature was recorded for each situation.

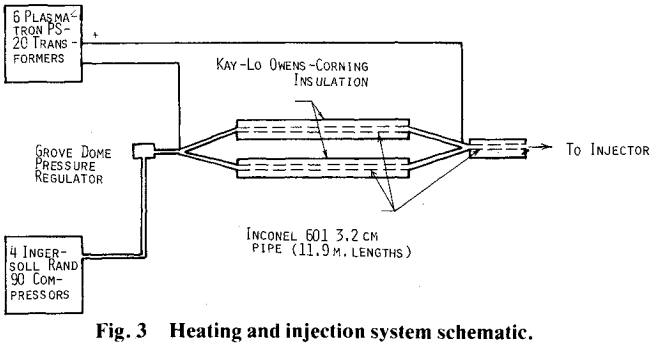

Fig. 3 Heating and injection system schematic.

Temperature fluctuations in the wake were measured using a straight hot wire (TSI model 1210). This probe was operated at a low overheat ratio of 1.05 in order to measure the temperature fluctuations more accurately. The probe was calibrated first by immersing the hot wire into an ice bath and then into boiling water. The output was adjusted so that the measured voltage was 0.0 V at 0°C and 10 V at 100°C.

Boundary-Layer Probes

The Pitot rake was approximately 3.8 cm in total height, with one static probe at the top and 24 total pressure tubes at increasing distances up from the wall. The temperature field near the body was measured by means of a thermocouple suspended vertically from a traverse mount.

Experimental Methods

Uniform Velocity, Temperature-Stratified Approach Flow

The primary consideration was to define the control settings that would allow a nearly uniform velocity distribution downstream of the injector while maintaining $(T_i - T_\infty)$ as large as possible. The injector exit temperature was monitored by a thermocouple located 1.3 cm from the exit. Temperature and pressure scans were taken at a station 40.6 cm upstream of the submarine body. The velocity defect or overshoot was observed and appropriate adjustments were then made to the pressure regulator ahead of the heating system. The final injection conditions selected were a U_i/U_∞ of 1.3, $(T_i - T_\infty)$ of 66°C. Typical velocity and temperature profiles at the station 40.6 cm upstream of the submarine body are shown in Fig. 4. Note the greatly exaggerated scale for velocity variations. Precise lateral uniformity from the injector proved to be difficult to obtain. The basic magnitudes of the velocity and temperature profiles were laterally uniform, but the local maximums were often at different locations along the Y axis. This "undesigned" characteristic of the injector proved to be helpful, however, in tracing the wake flow.

Self-Propelled Condition

It was determined that a propeller rpm of 12,980 was needed to achieve the self-propelled status. This corresponds to an advance-diameter ratio (U_∞/ND) of 0.628.

Results

The experimental results are presented in the form of velocity and temperature profiles for each station examined.

The turbulence data were not corrected for the effect of flow angularity and the mean flow data were not corrected for the effect of turbulent fluctuations. The latter approximation is valid due to the relatively small turbulence levels in most of the wake region. Jakubowski[8] has found in recent tests that the error induced by not correcting the turbulence data for flow angle variations is less than 7% for the flow angles encountered in this research.

Body Boundary-Layer Observations

The boundary-layer development along the body was examined in order to trace the temperature distribution in the longitudinal direction and subsequently to determine more accurately the effects of the propeller on the near-wake flowfield. Measurements were made with the Pitot rake and the thermocouple at $Z'/D = 2.67$, 4.67, 6.67, 8.67, and 10.0 on the side away from the "sail." By the station that was 10 diam. back from the model nose, the velocity boundary-layer thickness was about 2.5 cm.

Figure 5 contains the mean temperature distributions near the body at several streamwise stations. First, it should be noted that these distributions are not simply the thermal boundary layer, but rather that the thermal boundary layer is contained within the variable temperature region produced by the heated air injected upstream. The Prandtl number, which is the connecting link between the velocity and temperature fields, is near unity for air, which indicates that the velocity and temperature boundary layers should have nearly equivalent dimensions. The temperature varied over a distance of nearly double that of the velocity boundary layer. This is simply a result of the initial injection geometry and subsequent spreading of the jet. The development of the thermal boundary layer can be qualitatively examined by focusing attention on the region nearest the wall. Note that these profiles resemble a classical insulated wall thermal boundary layer. The regions wherein $dT/dy \approx 0$ can be seen to grow very distinctly with increasing Z'/D to the point that the size of the region at $Z'/D = 10$ is nearly twice that at station $Z'/D = 4.67$.

Figure 5 also shows the decay of the maximum of the high-temperature layer with increasing streamwise distance. This energy is lost to the freestream and manifests itself as a slow overall heating of the entire wind tunnel fluid.

Mean Wake Flow Observations

It was decided that an adequate description of the wake could be achieved with three traverses—vertical, horizontal, and 45 deg. The traverses were made in a quadrant opposite the "sail" and at downstream stations of $Z/D = 0.33$, 1.0, 2.0, 3.0, and 4.0.

Figures 6-8 are graphical presentations of the mean static pressure, mean axial velocity, and flow angularity distributions in the near wake at stations $Z/D = 0.33$, 2.0, and 4.0. At each station, results are presented along three traverses—vertical, horizontal, and diagonal.

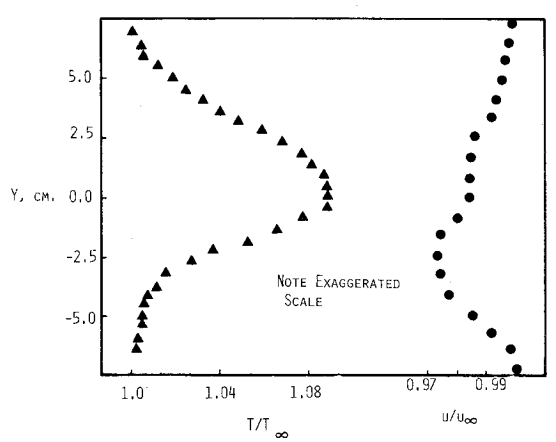

Fig. 4 Approach flow profiles.

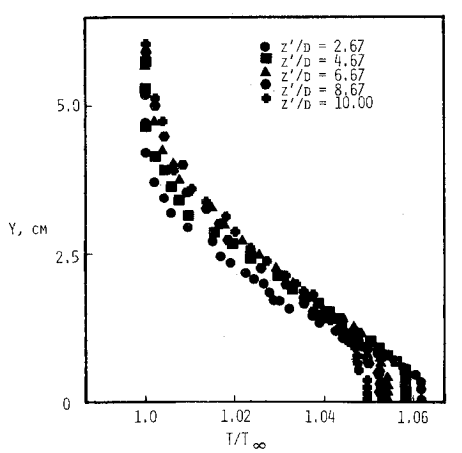

Fig. 5 Temperature profiles at various stations on the body.

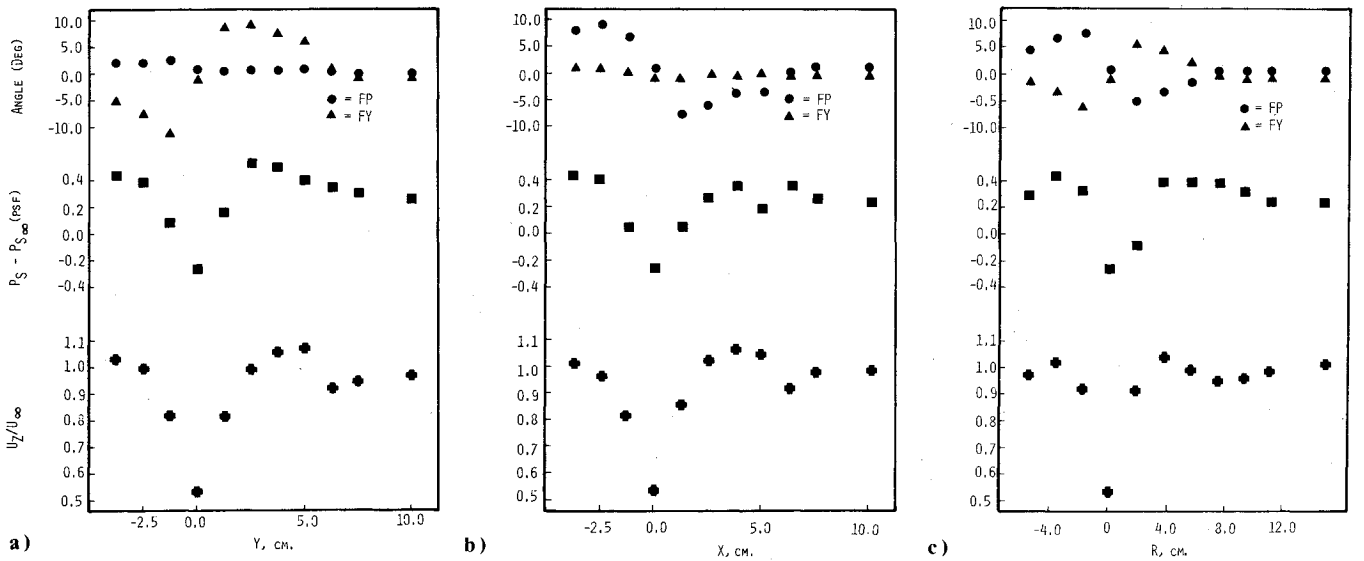

Fig. 6 Mean axial velocity flow, angularity and static pressure at $Z/D = 0.33$: a) vertical traverse, b) horizontal traverse, c) diagonal (45 deg) traverse.

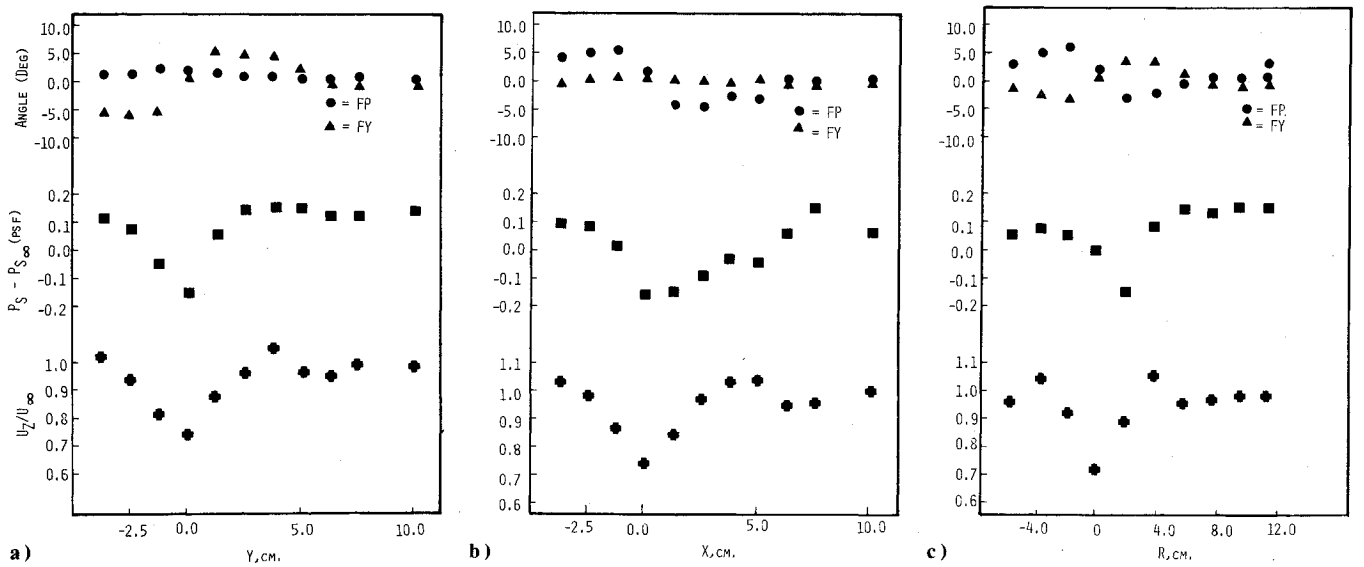

Fig. 7 Mean axial velocity flow, angularity and static pressure at $Z/D = 2.0$: a) vertical traverse, b) horizontal traverse, c) diagonal (45 deg) traverse.

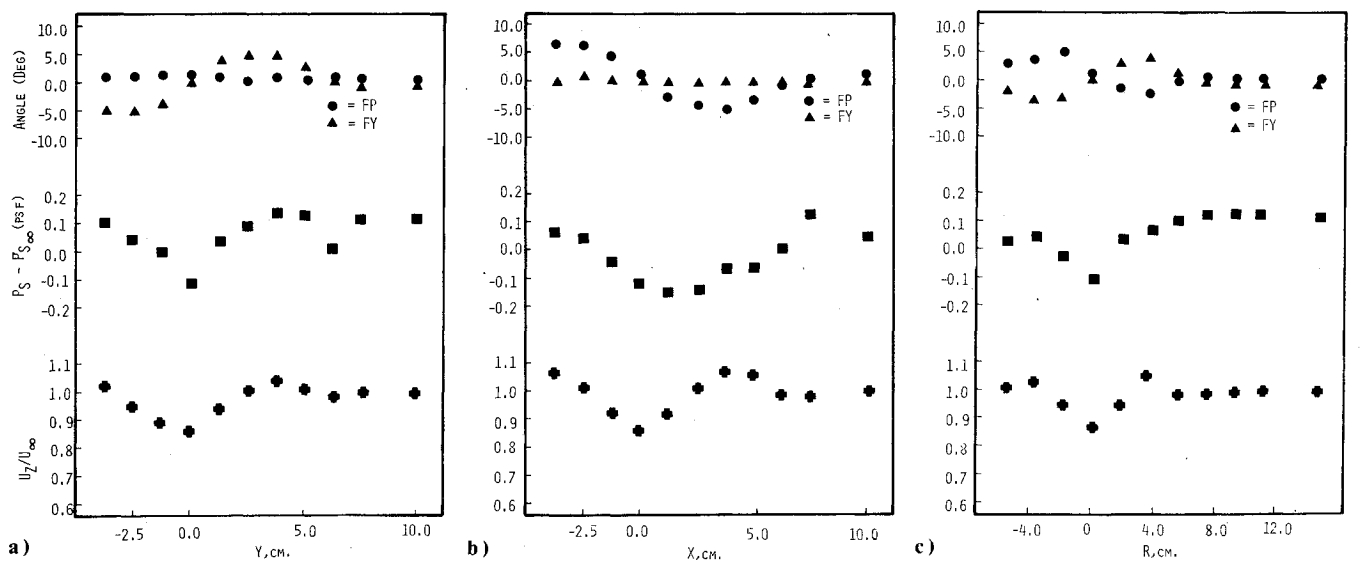

Fig. 8 Mean axial velocity flow, angularity and static pressure at $Z/D = 4.0$: a) vertical traverse, b) horizontal traverse, c) diagonal (45 deg) traverse.

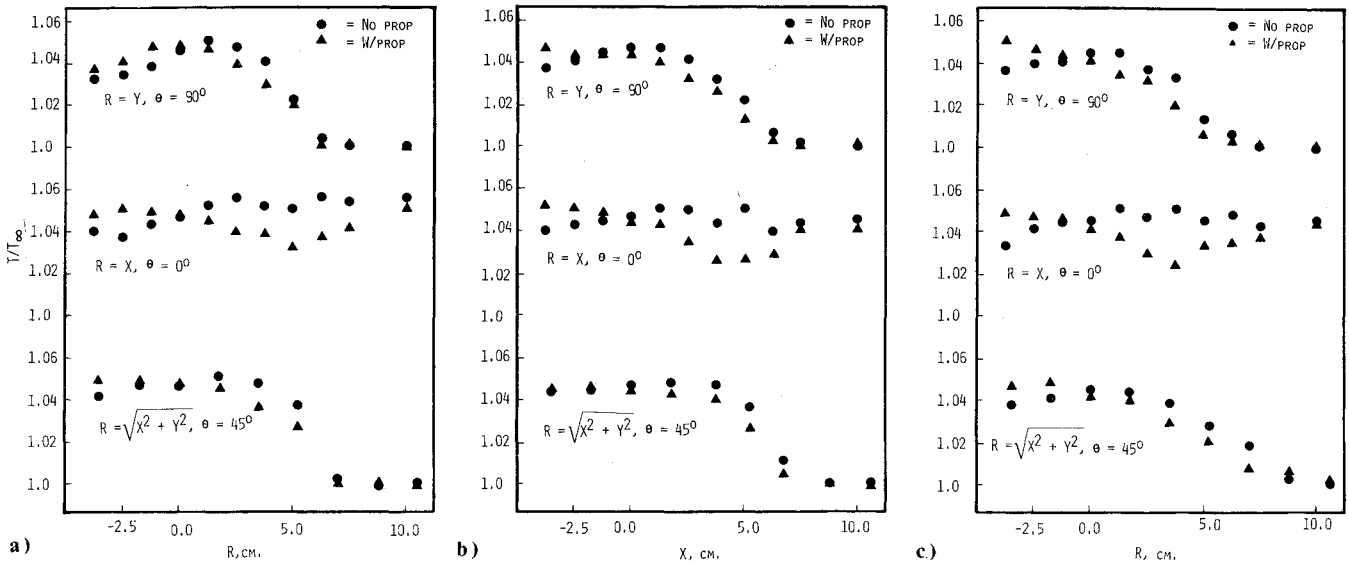

Fig. 9 Mean temperature distributions in the wake: a) $Z/D=0.33$, b) $Z/D=2.0$, c) $Z/D=40$.

From an overall examination of these data, one sees the initial momentum excess and defect regions spread in extent but decrease in magnitude with increasing Z/D. Similar behavior is exhibited by the propeller swirl and static pressure variations. Along a vertical traverse, the flow is pitched very slightly and the yaw angles are larger. The converse is true along the horizontal traverse. Maximum flow angles vary from approximately 10 deg at $Z/D=0.33$ to about 5 deg at $Z/D=4.0$.

Some small asymmetry of the results is evident. This is due to a combination of circumstances which cause the flow to deviate slightly from axisymmetric—the presence of the sail, the vertical and lateral gradients in the injected jet, and the small error in alignment which occurs in positioning the model.

Basically, the behavior of the flow is similar to that reported by Daffan.[5] The magnitude of the momentum excess and defect and the other associated properties of the wake structure are smaller due to the lower Reynolds number and corresponding lower propeller rpm of this study. One noticeable departure from the results of Ref. 5 is the appearance of a second momentum defect region in the near wake. At every station there is the maximum defect in the wake center. Passing the center there is a region of momentum excess characterized by the axial velocity overshoot. Continuing into the outboard portion of the wake, there is invariably another region of velocity defect which is smaller in both magnitude and extent. Actually, this behavior is predicted by simple propeller theory and is discussed in Ref. 9.

Of particular interest are the results in Figs. 9a-c. These are graphs of the temperature distribution in the wake at the stations used in obtaining the mean flowfield data. At each station, the three traverses were made, first with the prop not rotating and second at the rpm necessary to achieve the self-propelled condition. In the former circumstance, the prop was rotated out of the way by hand and positioned where it would not interfere with the flow.

The results at station $Z/D=0.33$ (Fig. 9a) are typical of each station if viewed singly. The initial temperature distribution without the influence of the propeller can be easily seen. The vertical variation is quite pronounced with peak temperatures of appoximately 9-11°C above T_∞. Ideally, the temperature variation along the horizontal traverse should be zero; however, variations up to 3°C are observed. This is largely due to the lateral gradients which were present initially in the injected jet and, to a lesser degree, to distortion produced by the body. The local temperature maximum at each lateral location along the jet injector were very nearly the same; however, the vertical location of these maximum would vary somewhat laterally.

Rotation of the propeller distorts the flow pattern. Look, for example, at the temperature distribution along the Y axis in the region from $Y=-3.8$ cm to 0.0 in Figs. 9a-c. One can clearly see an overall rotation of the flow as Z/D increases from 0.33 to 2.0 and finally 4.0. It is useful to attempt a crude numerical tracking of fluid particles as identified by mean temperature perturbations. Looking at the temperatures along the X axis in the region around $X=2.5$ cm in Figs. 9a-c, it appears that the higher temperature fluid particles present at $Z/D=0.33$ rotate to the $Y\approx-1.5$ region by the time $Z/D=4.0$. This postulated movement is, of course, consistent with the direction of rotation measured. The velocity and flow angularity data can be used to estimate how a given fluid particle rotates in the flow in the time Δt as it proceeds the 55.9 cm from $Z/D=0.33$-4.0. Unfortunately, the coarse "grid size" employed for the data collection prevents an exact analysis of the path of a particular streamline, but by taking the fluid state as it existed at station $Z/D=0.33$ and assuming that all gradients of the fluid properties are zero, one can very crudely estimate the location of these particles after Δt. Carrying out the calculations, the results are:

$$U_Y\approx-2.4 \text{ m/s}, \quad U_X\approx-0.4 \text{ m/s}, \quad \Delta t=0.03 \text{ s}$$

$$Y_1-Y_0=-3.8 \text{ cm}, \quad X_1-X_0=-1.0 \text{ cm}$$

These results indicate that the particles would move in pitch somewhat more than is observed and in yaw somewhat less than is observed. The discrepancies between the calculations and the observed results are due to the assumption of zero gradients in the flow properties. In fact, as the fluid particles move from the $+X$ axis to the $-Y$ axis, the pitch angles become smaller and the yaw angles become larger. This would result in a fluid element moving more in yaw and less in pitch than is crudely predicted by assuming $\partial U_x/\partial z$, $\partial U_y/\partial z=0$.

The propeller seems to act more as a "swirl inducer" than a "mixer" in this near-wake region. This is supported by the data, in that the levels of the maximum temperature observed do not fall more rapidly with distance downstream with the propeller activated than without. If a severe mixing action were occurring, one would expect a nearly uniform temperature to appear at these downstream locations with the propeller turning. That this is not the case indicates that there is a more or less fixed fluid element rotation occurring.

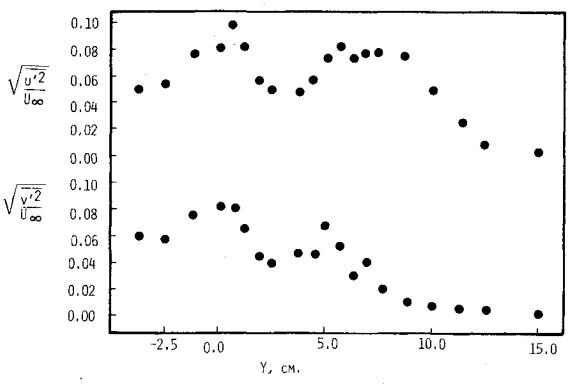

Fig. 10 Turbulence intensity distributions at $Z/D=0.33$, vertical traverse.

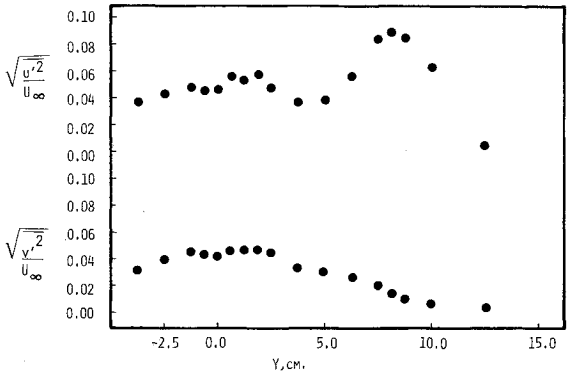

Fig. 11 Turbulence intensity distributions at $Z/D=4.0$, vertical traverse.

Turbulence Observations in the Wake

Turbulence measurements were performed in the near wake at stations $Z/D=0.33$ and 4.0. At each station, axial and radial turbulence intensities, radial shear stress, and temperature fluctuations were recorded.

Before discussing these data, a condition that existed which is detrimental to the accurate measurement with a hot wire should be pointed out. The injected air had a small oil content that was present because of leaky compressors. Examination of the hot-wire instruments after the tests revealed that small amounts of oil were deposited on the wires. It is probable that the electrical and thermal properties of the wires were changed somewhat by this deposit. Accordingly, the absolute levels of the reported fluctuations could be somewhat in error. Several measurements however, were duplicated at different times and with widely varying conditions such as compressor run-time (and thus oil vapor accumulation) and the data were seen to agree within 10%. This would indicate that the error due to the oil deposit is minimal.

Figure 10 shows that the axial velocity fluctuations are high (nearly 10% of the freestream velocity) at the center of the wake. The fluctuations decrease rapidly, followed by another peak which occurs in the vicinity of the propeller tips. At $Z/D=4.0$, Fig. 11 shows generally the same distribution, although the maximum intensities in the wake center have fallen to about half their former values. The radial turbulence intensity along all three traverses at $Z/D=0.33$ had the same distribution, with the maximums at the center of wake and at the propeller tips. However, at $Z/D=4.0$ the radial velocity fluctuation has fallen to 1-2% of the freestream velocity near the tips. The fluctuations along the center of the wake remain relatively high at 3-5%.

Figures 12 and 13 are graphs of the radial shear stress at stations $Z/D=0.33$ and 4.0, respectively. The data indicate that the highest values of the shear stress occur in the vicinity of high-velocity gradients, which is to be expected. The

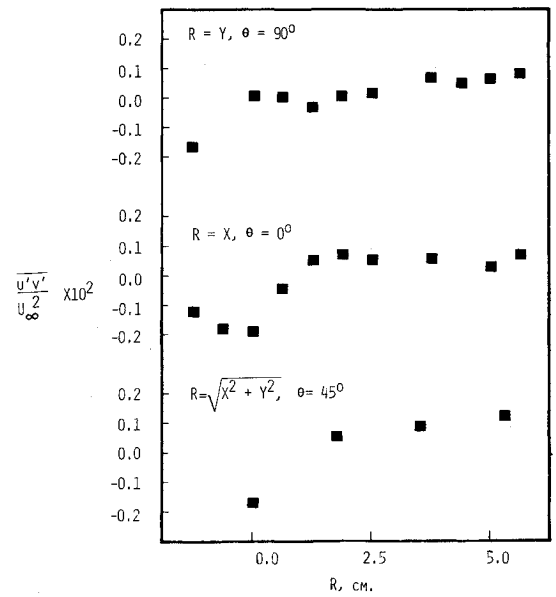

Fig. 12 Reynolds stress profiles at $Z/D=0.33$.

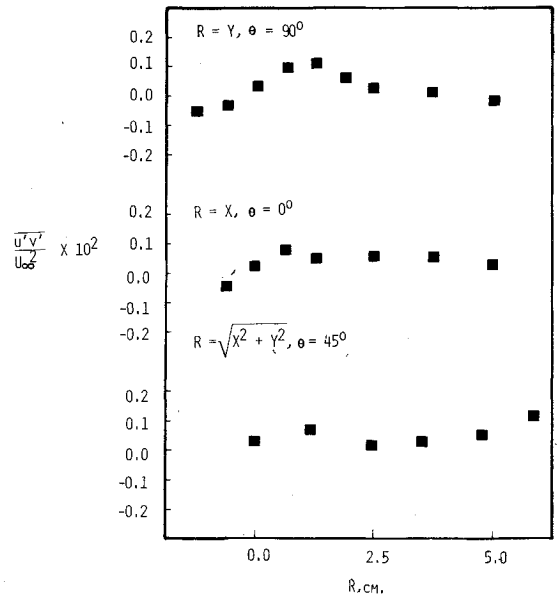

Fig. 13 Reynolds stress profiles at $Z/D=4.0$.

maximum values of the shear stress do not decrease greatly from $Z/D=0.33$-4.0.

Figure 14 is a graph of the temperature fluctuations at $Z/D=0.33$. These results show that the fluctuations are uniformly very small along any traverse until the edge of the wake is approached. The temperature fluctuations in this region are a maximum of approximately 2% along the horizontal and diagonal traverses and a comparatively large 3% along the vertical axis. Comparison with the data at $Z/D=4.0$ in Fig. 15 shows the same behavior. The levels along the vertical axis in the vicinity of the propeller tips are larger. The results in Figs. 9b and 9c show that the mean temperature differences are higher in the vicinity of the center of the wake and much smaller at the edge. The turbulence results indicate that the maximum temperature fluctuations are occurring in a region of relatively low mean temperature gradients. This is an important result when considered in the light of current turbulent transport modeling efforts. Such models generally indicate a strong production of temperature fluctuations due to mean temperature gradients, and that is

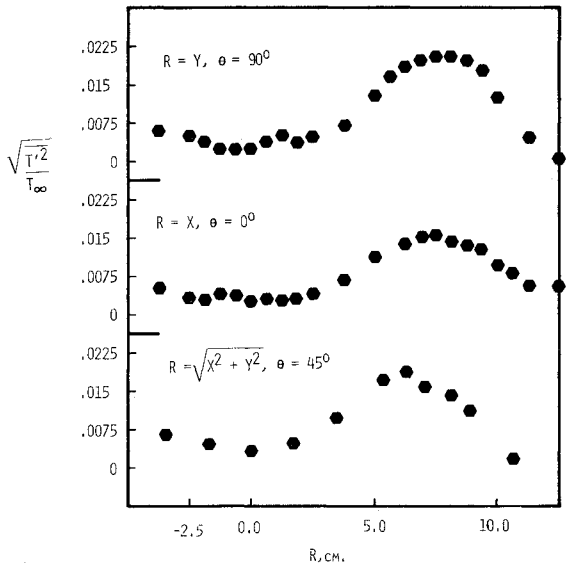

Fig. 14 Temperature fluctuation distributions at $Z/D = 0.33$.

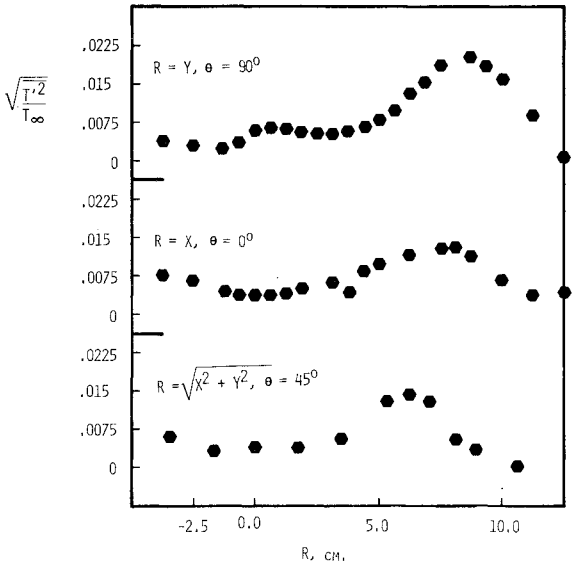

Fig. 15 Temperature fluctuation distributions at $Z/D = 4.0$.

not confirmed by the data for the present experimental situation.

It is tempting to try to relate the temperature fluctuations measured in the regions of small mean temperature differences previously discussed to the vortices shed from the rotating propeller blades. Our measurements of the rms values of T' cannot distinguish between turbulence and any cyclic unsteadiness in the flow from the rotating propeller. However, a cyclic unsteady velocity disturbance simply cannot directly produce a temperature fluctuation in a nearly constant temperature region.

Conclusions and Recommendations

An experimental study of the flowfield produced by a self-propelled, slender body of revolution in a temperature-stratified airstream has been conducted. The experiments concentrated mainly on the mean and turbulent flow in the near-wake region, although mean boundary-layer measurements were taken in order to establish the initial conditions immediately upstream of the propeller.

The mean flow results have shown that the temperature stratification used in this experiment had no large, explicit effect on the development of the mean flow in the near wake. This is a result of the high Froude number. The temperature results show that the fluid undergoes a rather simple rotation in this near-wake region and that there is no great increase in mixing rate produced by the propeller.

The turbulence measurements reinforce recent findings that the highest levels of axial turbulence intensity are to be found in the immediate vicinity of the propeller tips. Additionally, the current results indicate that higher levels of turbulence than previously found are present in the wake center. These centerline fluctuations appear to decay at a faster rate than do the turbulence intensities at the outboard edge. They are, possibly, only a phenomenon peculiar to the very near-body region, and our results here are closer to the propeller than those previously reported. The radial turbulence intensities are also unusually high at the wake center. In fact, in this case, the magnitudes along the centerline are higher than those near the propeller tips at the most distant downstream station studied.

The turbulent temperature fluctuations measured were mainly significant only near the radial location of the propeller blade tips. Interestingly, large fluctuations were also found to be present at circumferential locations where the mean temperature field was nearly uniform.

The results suggest some interesting points for further study. The influence of different initial mean temperature distributions should be determined. The temperature fluctuation distribution in the vicinity of the propeller tips is quite pronounced, and it would be interesting to see the effect of different initial temperature gradients and their location relative to the propeller geometry. Second, the turbulent thermal boundary layer should be probed, since the incoming turbulence levels can be expected to have direct effects on the wake development.

Acknowledgment

This work was supported by Advanced Research Projects Agency. P. Selwyn of The Institute for Defense Analysis was the Technical Monitor.

References

[1] Naudascher, E., "Flow in the Wake of a Self-Propelled Body and Related Sources of Turbulence," *Journal of Fluid Mechanics*, Vol. 22, 1965, pp. 625-656.

[2] Gran, R. L., "An Experiment on the Wake of a Slender Propeller-Driven Body," TRW Rept. 20086-6006-RU-80.

[3] Swanson, Jr., R. C., Schetz, J. A., and Jakubowski, A. K., "Turbulent Wake Behind Slender Bodies Including Self-Propelled Configurations," VPI-AERO-024, 1974; available through D.D.C.

[4] Chieng, C. C., Jakubowski, A. K., and Schetz, J. A., "Investigation of the Turbulent Properties of the Wake Behind Self-Propelled Axisymmetric Bodies," VPI-AERO-025, 1974; available through D.D.C.

[5] Daffan, E. B., "Mean Flow and Turbulence Measurements in the Wake of a Slender Propeller-Driven Body Including Effects of Pitch Angle," M.S. Thesis, Virginia Polytechnic Institute and State University, Blacksburg, Va., 1976.

[6] Schetz, J. A., Daffan, E. B., Jakubowski, A. K., Cannon, S., Cox, R., and Dubberley, D., "Mean Flow and Turbulence Measurements in the Wake of Slender Propeller-Driven Bodies Including Effects of Pitch Angle," VPI-AERO-050, 1976; available through D.D.C.

[7] Hokenson, G. J., "Incompressible Free Turbulent Mixing in Axial Pressure Gradients," Ph.D. Dissertation, University of Maryland, College Park, Md., 1970.

[8] Jakubowski, A. K., private communication, Feb. 1977.

[9] Durand, W. F., *Aerodynamic Theory*, Vol. IV, Dover Publications, Inc., New York, N.Y., 1963.